

## INTERNAL FLOW CHARACTERISTICS OF A CENTRIFUGAL PUMP WITH VERY LOW SPECIFIC SPEED

*Young-do CHOI,*

*Yokohama National University,*

*Junichi KUROKAWA,*

*Yokohama, Japan*

*Jun MATSUI,*

*Hiroshi IMAMURA,*

### ABSTRACT

In the very low specific-speed range ( $N_s < 100$  [m, m<sup>3</sup>/min, rpm]), the efficiency of turbo-pump designed by conventional method becomes remarkably low. Therefore, positive-displacement pumps have long been used widely. However, the positive-displacement pumps have problems such as noise, vibration and need high manufacturing precision. Recently, since the turbo-pumps are becoming higher in rotational speed and smaller in size, there are lots of expectation of developing new turbo-pump with high performance at the very low specific speed range. The purpose of this study is to investigate the internal flow characteristics of a centrifugal pump in order to improve the pump performance. The results show that there is large recirculation flow at semi-open impeller outlet and the pump performance is largely affected by this recirculation flow.

### RÉSUMÉ

Dans le domaine des vitesses spécifiques très basses ( $N_s < 100$  [m, m<sup>3</sup>/min, t/min]), le rendement des turbopompes conçues de manière conventionnelle devient extrêmement faible. De ce fait, des pompes volumétriques ont été largement utilisées. Cependant, les pompes volumétriques pressentent des problèmes tels que bruit ou vibrations, et nécessitent une précision élevée lors de la fabrication. Comme les turbopompes deviennent de plus en plus rapides en vitesse de rotation et compactes en dimensions, il y a beaucoup d'espoir de développer de nouvelles pompes de haute performance à faible vitesse spécifique. Le but de cette étude est d'examiner les caractéristiques de l'écoulement interne dans une pompe centrifuge afin d'en améliorer les performances. Les résultats montrent la présence de larges zones de recirculation en sortie de roues semi-ouvertes et que les performances en sont largement affectées.

### NOMENCLATURE

Term	Symbol	Definition	Term	Symbol	Definition
Specific speed	$N_s$	[m, m <sup>3</sup> /min, rpm]	Impeller radius	$r$	[mm]
Flow coefficient	$\varphi$	$Q / (A u_2)$	Tip clearance ratio	$\lambda$	$c/b_2$
Head coefficient	$\psi$	$[H / (u_2^2/2g)]$	Tip clearance	$c$	[mm]
Power coefficient	$\nu$	$[P / (\rho A_2 u_2^3)]$	Impeller width	$b$	[mm]
Flow rate	$Q$	[m <sup>3</sup> /min]	Impeller tip speed	$u$	[m/s]
Recirculation flow	$q_s$	[m <sup>3</sup> /min]	Impeller blade number	$z$	
Head	$H$	[m]	Revolution number	$n$	[rpm]
Slip factor	$k$	$(V_{\theta 2\sigma} - \bar{V}_{\theta 2}) / U_2$	Reynolds number	$R_e$	$\rho u_2 r_2 / \mu$
Impeller blade angle	$\beta$	[deg.]	Impeller inlet / outlet	1 / 2	Subscripts

## INTRODUCTION

Positive-displacement pumps have long been used widely in the range of very low specific speed. However, because of, not only, the problems such as noise, vibration and high manufacturing precision, but also, the recent trend of small size-high speed, application of turbo-pump to the very low  $N_s$  range is strongly expected. However, efficiency of a centrifugal pump decreases rapidly with a drop of specific speed (Ref. 1). Kurokawa et al. revealed that the low efficiency of a very low  $N_s$  impeller is mainly caused by large disc friction (Ref. 2). And they also have estimated and proposed the design guideline of high performance pump at the very low specific speed  $N_s = 60$  (Ref. 3). Besides, more detailed information of internal flow characteristics is required in order to develop new centrifugal pump with high performance at the range of a very low  $N_s$ . The present paper describes the results of numerical simulation and experimental measurement of internal flow characteristics in a very low specific speed centrifugal pump.

## APPARATUS AND EXPERIMENTAL AND NUMERICAL METHOD

The schematic view and dimensions of the impellers tested are given in Fig. 1 and Table 1. Eight kinds of impeller were employed to investigate the internal flows. Closed impeller C1 is designed by a conventional method (Ref. 1) and operated on the free impeller condition which includes parallel walled channel around the impellers and there is no volute casing. The axial symmetry of the impeller flow is confirmed by constant pressure distribution around the impeller outlet. Semi-open impeller S1 and S2, which is made of transparent acrylic resin, is adopted for a visualization pump (with volute). This pump is manufactured for PIV (Particle Image Velocimetry) measurement and have two-dimensional configuration. Suction cover and volute casing are made of transparent acrylic resin. Double-pulsed Laser sheet enters the pump in a direction tangential to the test impeller. Closed impeller C2 and semi-open impeller S3, S3', S4 and S4' are used for tip clearance variation test. The volute pump for tip clearance variation test has a suction cover which is made of transparent acrylic resin in order to conduct LDV (Laser-Doppler Velocimetry) measurement and can be displaced in the axial direction for tip-clearance adjustment.

Table 1 Dimensions of test impellers

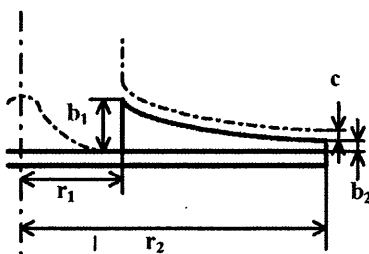


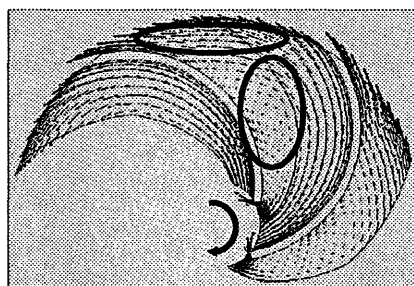
Fig. 1 Schematic view of test impeller

Impeller	C1	C2	S1	S2	S3	S3'	S4	S4'
Type	Close d	Close d	Semi-open	Semi-open	Semi-open	Semi-open	Semi-open	Semi-open
$\beta_1$	27.2	20.5	90	22.5	20.5	20.5	20.5	20.5
$\beta_2$	22.5	60	90	30	60	60	60	60
$b_1$	16	10	8	8	10	10	15.4	15.4
$b_2$	4	2	8	8	2	2.25	8	9
$r_1$	27.5	26	16	16	26	26	26	26
$r_2$	130	101	60	60	101	91	101	91
$z$	5	6	6	4	6	6	6	6
$n$	750	3000	700	700	3000	1500	3000	1500
$\Phi_0$	0.0692	0.0714	0.0004	0.0004	0.0714	0.0714	0.0179	0.0179
$Re$	$3.0 \times 10^8$	$3.02 \times 10^8$	$6.0 \times 10^7$	$6.0 \times 10^7$	$3.02 \times 10^8$	$2.92 \times 10^8$	$3.02 \times 10^8$	$2.9 \times 10^8$
$N_s$	84	57.5	100	100	57.5	57.5	57.5	57.5

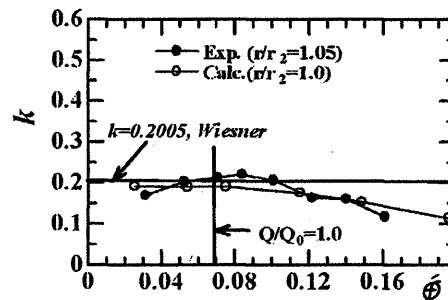
For the numerical analysis of the impeller internal flows, commercial code TASCflow is used. Governing equation is 3-dimensional Reynolds averaged Navier-Stokes equation which was discretized by finite volumetric method. Modified LPS scheme is used for discretization of a convection term. Also,  $k-\omega$  model is adopted for a turbulence model. Computational grid consists of one flow passage for each test impeller.

### INTERNAL FLOW OF CLOSED TYPE FREE IMPELLER (C1)

Calculated results of relative velocity vectors and slip factor of closed impeller C1 are shown in Fig. 2. Definite distinction of a very low  $N_s$  closed impeller C1 in comparison with a normal  $N_s$  impeller (Ref. 1) is extremely narrow outlet width ( $b_2=4$ [mm]). Fig. 2(a) reveals that there is a large vortex flow zone along the blade pressure side in the impeller passage and strong secondary flow runs from blade suction side to pressure side at the vicinity of impeller outlet even at design flow rate. This flow pattern is similar to that of potential flow and different from the flow in the normal  $N_s$  impeller (Ref. 4). Similar result has been reported by other researchers (Ref. 5). The reason of complex flow is considered to be caused by strong wall friction on the both surfaces of front and main shroud. By the wall friction, Coriolis force becomes weak in the vicinity of both walls. Flow is extremely deflected to pressure side by the effect of Coriolis force at the middle plane of blade width. Consequently, even at design flow rate, there exists strong secondary flow and vortex flow zone between the flow passage. Also, Kurokawa et al. have found that the best efficient point of impeller C1 is located at about 200% of the design point (Ref. 2). Slip factor shows that the result of calculation agree well with that of experiment and Wiesner (Ref. 4) at the design point.



(a) Relative vectors ( $Q/Q_0=1.0$ )

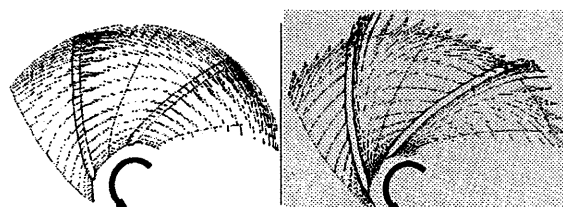


(b) Slip factor

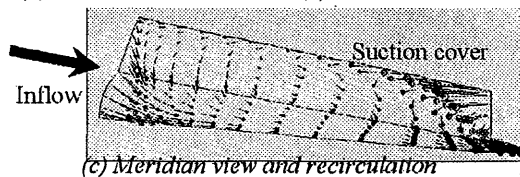
Fig. 2 Very low specific speed closed impeller C1 ( $N_s=84$ , no volute)



Fig. 3 Measured relative velocity vectors of a Semi-open impeller S1 ( $N_s=100$ ,  $Q/Q_0=0.25$ )



(a) Near to suction cover (b) Near to main shroud



(c) Meridian view and recirculation

Fig. 4 Calculated relative velocity vectors of a semi-open impeller S3' ( $N_s=57.5$ ,  $Q/Q_0=1.0$ ,  $\lambda_2=4.0$ )

### RELATIVE VELOCITY VECTORS OF A SEMI-OPEN IMPELLER (S1, S3')

Relative velocity vectors of semi-open impellers S1 and S3' are shown in Fig. 3 and 4, respectively. Fig. 3 is the result of PIV measurement. There are strong reverse flow at the outlet of semi-open impeller S1 ( $N_s=100$ ). Moreover, a large vortex flow zone is formed at the pressure side of impeller outlet at low flow rate  $Q/Q_0=0.25$  (Fig. 3). The vortex disappears gradually as flow rate increases but the reverse flow remains regardless of flow rate. Fig. 4(c) shows calculated relative velocity vectors of meridian cross sectional plane for the case of large tip clearance  $\lambda_2=4.0$ , and reveals that there exists a strong recirculation flow. This recirculation flow causes a large difference of flow pattern between a semi-open impeller (Fig. 4(a)&(c)) and a closed impeller (Fig. 2(a)). There exist strong reverse flow at tip clearance (Fig. 4(a)) and outflow at the side of main shroud (Fig. 4(b)) in the very low  $N_s$  semi-open impeller. According to the numerical simulation, the recirculation flow zone becomes larger at impeller outlet as tip clearance ratio increases.

### CHANGE OF PERFORMANCE CURVES AS PER TIP CLEARANCE RATIO

Performance curves of a volute pump as per the variation of tip clearance ratio is shown in Fig. 5. Design specific speed of the test impeller is  $N_s=57.5$ . As tip clearance ratio decreases, head becomes higher with an increase of efficiency. However, simultaneously, performance instability, which is characterized by the increasing head curve as per the increase of flow rate, increases. Accordingly, with appropriate tip clearance ratio, semi-open impeller can be applied to the countermeasure of performance instability of closed impeller. Fig. 6 indicates that as tip clearance ratio decreases, the best efficiency and the design point efficiency increases at the same time. And each efficiency of the impellers as per tip clearance ratio can be expressed in one curve with gentle gradient and saturates in the range of  $\lambda_2 > 2$ .

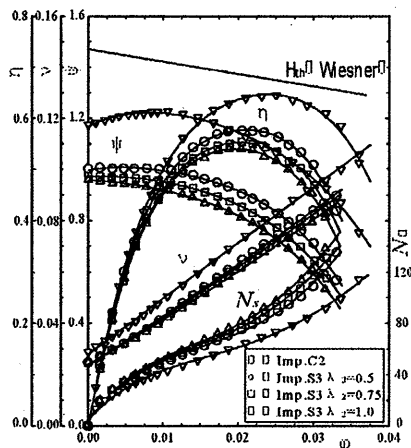


Fig. 5 Performance curves

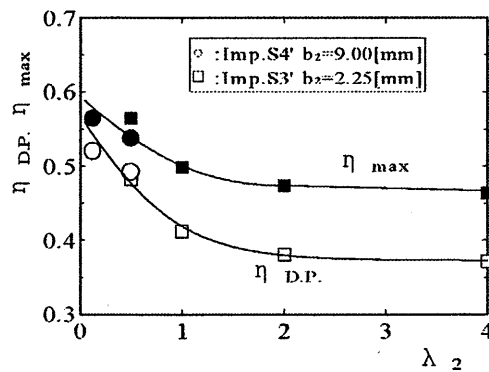
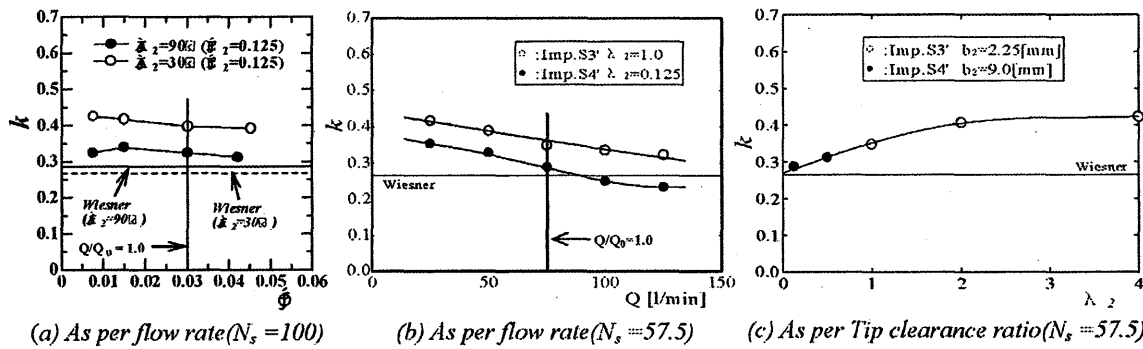


Fig. 6 Efficiency variation to tip clearance ratio



(a) As per flow rate ( $N_s = 100$ ) (b) As per flow rate ( $N_s = 57.5$ ) (c) As per Tip clearance ratio ( $N_s = 57.5$ )

Fig. 7 Slip factor of very low  $N_s$  semi-open impellers as per flow rate and tip clearance ratio

### SLIP FACTOR OF SEMI-OPEN IMPELLERS

Slip factor of very low  $N_s$  semi-open impeller is shown in Fig. 7 against the variation of flow rate and tip clearance. Slip factor of conventional closed impeller is known to agree well with the value of Wiesner regardless of flow rate (Ref. 7). However, the slip factor of very low  $N_s$  semi-open impeller is larger than that of Wiesner through whole flow rate as shown in Fig. 7. While, slip factor of very low  $N_s$  semi-open impeller increases according to the increase of tip clearance ratio as shown in Fig. 7(b). Fig. 7(c) reveals that the inclination of the slip factor become flat at  $\lambda_2 > 2$  and, as tip clearance ratio goes to zero, the slip factor becomes same as that of closed impeller. The tendency of slip factor for the change of tip clearance ratio is almost same as that of efficiency in the very low  $N_s$  semi-open impeller as shown in Fig. 6. Accordingly, it is considered that the slip factor of very low  $N_s$  semi-open impeller has dominating effect on the performance of impeller.

### RECIRCULATION FLOW AND PERFORMANCE ESTIMATE

As shown in Fig. 5, the head and efficiency curves of a closed impeller C2 is much higher than that of a semi-open impeller S3, though the configuration is same except for the front shroud. The theoretical heads of both impellers are same. And, the difference of slip factor is not large as is revealed by Fig. 7(c). The large difference of head curve should be caused by the difference of impeller outlet flow, that is the absolute peripheral velocity. To examine this, the radial distribution of the absolute circumferential velocity was measured. In Fig. 8, the measured circumferential velocity is plotted against radius, together with the data of normal  $N_s$  impeller (Ref. 6). In case of normal  $N_s$  impeller (both closed and semi-open), absolute circumferential velocity ratio to the impeller radius increases gradually from impeller inlet to outlet and the velocity decreases steeply just after coming out the impeller outlet (Ref. 6). However, very low  $N_s$  semi-open impeller has different velocity distribution depending on specific speed  $N_s$ . The velocity distribution of impeller S1 ( $N_s=100$ ) indicates that absolute circumferential velocity at impeller inlet is higher than that of normal  $N_s$  impeller and the gradual increment of velocity distribution changes to steep decrement after the radius ratio  $r/r_2=0.8$ . The difference of velocity distribution become more deviated from normal  $N_s$  impeller in case of very low specific speed impeller S4' ( $N_s=57.5$ ). The velocity distribution of impeller S4' is flat from impeller inlet and decrease steeply after  $r/r_2=0.8$ . It is considered that the steep decline of circumferential velocity at the outlet of very low  $N_s$  impeller and high absolute circumferential velocity ratio in the impeller flow passage result from the effect of large recirculation shown in Fig. 4(c). This recirculation flow takes low

angular momentum into impeller passage and reduce the angular momentum of outlet flow largely.

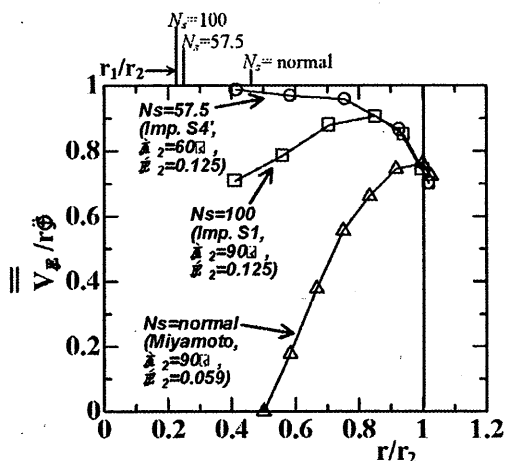
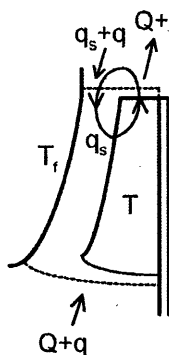
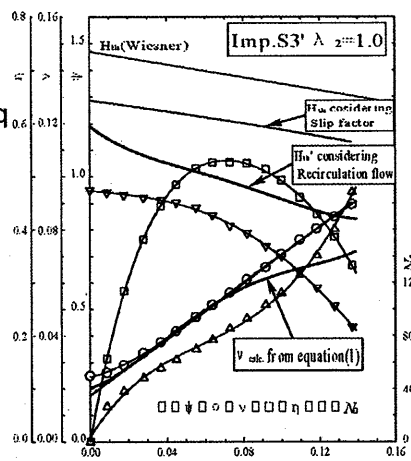


Fig. 8 Absolute circumferential velocity ratio



(a) Recirculation flow



(b) Performance curves

Fig. 9 Recirculation flow and performance of a very low  $N_s$  semi-open impeller

In order to determine the recirculation flow effect on the head curve of a semi-open impeller, the outlet flow pattern is modeled as shown in Fig. 9(a). Using the recirculation flow rate  $q_s$ , the angular momentum balance in the control volume in Fig. 9(a) is expressed as

$$T - T_f + \rho(q_s + q)v_{\theta}r_2 = \rho(Q + q_s + q)(v_{u2}r_2 - v_{u1}r_1) \quad (1)$$

where  $T$  is supplied torque,  $T_f$  is a friction torque consumed by a front shroud,  $\rho$  is density of fluid,  $q$  is leakage flow and  $v_{u2}$  is circumferential velocity of impeller outflow. Putting  $\alpha = q_s/(Q+q)$ , the theoretical head of semi-open impeller  $H_{th}'$  is expressed using  $H_{th}$  of a closed impeller as below.

$$H_{th}' = \frac{H_{th}}{1+f\zeta} + \frac{f\zeta}{1+f\zeta} \cdot \Delta H_{th}, \quad \text{where } \Delta H_{th} = u_2(v_{u2} - v_{u2}') \quad (2)$$

where  $v_{u2}'$  is circumferential velocity of recirculation flow at impeller outlet. The above-obtained theoretical head  $H_{th}'$  of a semi-open impeller and the power induced by equation (1) are shown in Fig. 9(b). Except for high and partial flow rate, there is good agreement between input power and calculated power. Consequently, the reason of performance difference between a semi-open impeller and a closed impeller is concluded to the existence of recirculation flow at semi-open impeller outlet.

## CONCLUSION

1. The main difference of performance between semi-open impeller and closed impeller in the range of very low  $N_s$  results from recirculation flow at the outlet of semi-open impeller. The recirculation flow causes the performance drop of semi-open impeller in case of large tip clearance ratio.
2. In the semi-open impeller, slip factor differs from that of closed impeller. The slip factor of semi-open impeller is higher than that of conventional normal  $N_s$  closed impeller. Additional slip due to a recirculation flow is proposed.

3. Slip factor and pump efficiency are just related to tip clearance ratio, not to blade width in a semi-open impeller. As the tip clearance increases, there are increase of slip factor and decrease of efficiency. However, there exist constant value of slip factor and efficiency regardless of tip clearance increase at the range of tip clearance ratio larger than 2.0.

## ACKNOWLEDGEMENT

The authors wish to express their appreciation to Prof. K. Nishino of Y.N.U. for his support on PIV measurement and to Mr. M. Ishii for conducting LDV measurement.

## REFERENCES

- Ref. 1 Stepanoff, A. J., 1957, "Centrifugal and Axial Flow Pumps(2nd ed.)", John Wiley and Sons, pp. 69-89.
- Ref. 2 Kurokawa, J., et al., 1997, "Performance of Very Low Specific Speed Impeller (in Japanese) ", Turbomachinery, Vol.25, pp.337-345.
- Ref. 3 Kurokawa, J., et al., 2000, "Study on Optimum Configuration of a Volute Pump of Very Low Specific Speed (in Japanese)", Trans. JSME, B, Vol.66, pp.1132-1139.
- Ref. 4 Murakami, M., et al., 1980, "Velocity and Pressure Distributions in the Impeller Passages of Centrifugal Pumps", Trans. ASME, Vol.102, December, pp.420-426.
- Ref. 5 Abramian, M., Howard, J. H. G., 1994, "Experimental Investigation of the Steady and Unsteady Relative Flow in a Model Centrifugal Impeller Passage", Trans. ASME, J. Turbomachinery, Vol.116, April, pp.269-279.
- Ref. 6 Miyamoto, H., Ohba, H., 1993, "The Effect of Flow Rate on Characteristics in Centrifugal Impellers (in Japanese)", Trans. JSME, B, Vol.59, pp.468-472.
- Ref. 7 Wiesner, F. J., 1967, "A Review of Slip Factors for Centrifugal Impellers, Trans. ASME, Ser.A., 89-4, October, pp.558-572.